Am J Transl Res 2020;12(11):7144-7159
www.ajtr.org /ISSN:1943-8141/AJTR0114562

Original Article

Uremic toxic substances are essential elements for enhancing carotid artery stenosis after balloon-induced endothelial denudation: worsening role of the adventitial layer

Jiunn-Jye Sheu[1], Chih-Chao Yang[2], Christopher Glenn Wallace[3], Kuan-Hung Chen[4], Pei-Lin Shao[5], Pei-Hsun Sung[6], Yi-Chen Li[6], Yi-Ching Chu[6], Jun Guo[7], Hon-Kan Yip[5,6,8,9,10,11]

[1]Division of Thoracic and Cardiovascular Surgery, Department of Surgery, Kaohsiung Chang Gung Memorial Hospital and Chang Gung University College of Medicine, Kaohsiung 83301, Taiwan; [2]Division of Nephrology, Department of Internal Medicine, Kaohsiung Chang Gung Memorial Hospital and Chang Gung University College of Medicine, Kaohsiung 83301, Taiwan; [3]Department of Plastic Surgery, University Hospital of South Manchester, Manchester, United Kingdom; [4]Department of Anesthesiology, Kaohsiung Chang Gung Memorial Hospital and Chang Gung University College of Medicine, Kaohsiung 83301, Taiwan; [5]Department of Nursing, Asia University, Taichung 41354, Taiwan; [6]Division of Cardiology, Department of Internal Medicine, Kaohsiung Chang Gung Memorial Hospital and Chang Gung University College of Medicine, Kaohsiung 83301, Taiwan; [7]Department of Cardiology, The First Affiliated Hospital, Jinan University, Guangzhou 510630, China; [8]Institute for Translational Research in Biomedicine, Kaohsiung Chang Gung Memorial Hospital, Kaohsiung 83301, Taiwan; [9]Center for Shockwave Medicine and Tissue Engineering, Kaohsiung Chang Gung Memorial Hospital, Kaohsiung 83301, Taiwan; [10]Department of Medical Research, China Medical University Hospital, China Medical University, Taichung 40402, Taiwan; [11]Division of Cardiology, Department of Internal Medicine, Xiamen Chang Gung Hospital, Xiamen 361028, Fujian, China

Received May 18, 2020; Accepted October 9, 2020; Epub November 15, 2020; Published November 30, 2020

Abstract: This study tested the hypothesis that uremic-toxic substances play a crucial role in enhancing left-common carotid artery (LCCA) stenosis after balloon-denudation of LCCA endothelium (BDLCCAE), and that the adventitial layer plays a complementary role in worsening LCCA stenosis. *In vitro* results showed the protein expressions of inflammation (IL-1β/TNF-α/IL-6), apoptosis (mitochondrial-Bax/cleaved-caspase-3/cleaved-PARP) and autophagy (beclin/Atg5/LC3B-II to LC3B-I ratio) as well as protein (NOX-1/NOX-2/p22phox/oxidized-protein), total cellular (H2DCFDA) and mitochondrial (Mitosox) levels of oxidative stress were significantly increased in p-Cresol-treated umbilical vein endothelial cells (HUVECs) as compared with control, whereas angiogenesis capacity (i.e., Matrigel-assay for HUVECs) exhibited an opposite pattern to inflammation between the two groups (all $P < 0.001$). Animals (n = 60) were categorized into group 1 (sham-operated control), group 2 (BDLCCAE), group 3 [BDLCCAE + ESRD patient's serum (1 cc/injection into deprived CA adventitia)], group 4 [BDLCCAE + ESRD patient's serum (1 cc/injection from peri-adventitia)], and group 5 [BDLCCAE + ESRD patient's serum (2 cc/by intravenous injection at days 1/3/7/10/14 after BDLCCADE)] and LCCA was harvested by day-21 after BDLCCAE procedure. Nitric-oxide release from LCCA and the LCCA cross-section area significantly and progressively reduced, whereas intimal and medial layers of LCCA significantly and progressively increased from groups 1 to 5 (all $P < 0.001$). The cellular expressions of inflammation (CD14+) and DNA-damage biomarker (γ-H2AX+) were significantly and progressively increased, whereas endothelial surface markers (CXCR4/vWF+) were significantly and progressively reduced from groups 1 to 5 (all $P < 0.0001$). Uremic toxins played an essential role in LCCA remodeling and obstruction. LCCA adventitia facilitated the initiation and propagation of LCCA proliferative obstruction.

Keywords: Denudation of carotid artery endothelium, adventitia, uremic toxic substances, stenosis, inflammation, oxidative stress

Introduction

Atherosclerosis, caused by the initiation and propagation of endothelial dysfunction, propagates into atheromatous plaque formation and ultimately develops into plaque rupture and arterial obstructive syndrome (AOS) [1-8]. Hypertension, hypercholesterolemia, smoking,

diabetes mellitus and uremic toxic substances are risk factors for endothelial dysfunction and atherosclerosis [9-13]. Of these, accumulated uremic toxic substances from end stage renal disease (ESRD) is an important risk factor for endothelial dysfunction, plaque formation and AOS [12, 13] with the poorest response to medication and coronary artery interventions (including catheter-based interventions and coronary artery bypass surgery) [13-21], resulting in poor long-term prognosis and unacceptably high morbidity and mortality [19-22].

Circulatory endothelial progenitor cells (EPCs) play a crucial role in reendothelialization and vascular endothelial repair from damage or endothelial senescence [23-25]. The number and function of EPCs are depleted in chronic kidney disease (CKD) and end-stage renal disease (ESRD) patients [26-28], highlighting how AOS commonly occurs and why obstructed vessels are difficult to treat in these patients [18-22]. However, these data are mainly from clinical observational studies [12-28] that lack mechanistic investigations into how uremic toxic substances cause and compound AOS.

Basic research studies have revealed that resident stem/progenitor cells are present in adventitia and participate in vascular wall repair and formation of neointimal lesions in severely damaged vessels [29, 30], resulting in arteriosclerosis [31-33]. However, whether the adventitial layer of the carotid artery also participates in the stenosis of endothelium denuded left common carotid artery (LCCA), particularly when under uremic toxic stimulation, remains unknown.

The aforementioned issues [12, 13, 29-33] encouraged us to utilize an animal model of balloon denuded LCCA endothelium (BDLCCAE) to investigate the mechanisms of how uremic toxic substances may be involved in the elicitation and propagation of endothelial dysfunction, intimal and medial layer hyperplasia and LCCA stenosis as well as the potential for a complementary role of the adventitial layer on LCCA obstruction.

Materials and methods

Ethics

All animal procedures were approved by the Institute of Animal Care and Use Committee (Affidavit of Approval of Animal Use Protocol No. 2017050902. Animals were housed in our hospital with controlled temperature and light cycles (24°C and 12/12 light cycle).

Animal model of left common carotid artery injury by angioplasty balloon and animal groupings

The procedure and protocol were as previously described [34]. Adult male Sprague-Dawley (SD) rats (n = 60) (Charles River Technology, BioLASCO, Taiwan) were utilized in the current study. All animals were anesthetized by inhalation of 2.0% isoflurane for isolation of the left external and common carotid arteries in the neck.

A small opening was created over the proximal left external carotid artery with a scalpel after adequate exposure in sterile conditions. A coronary angioplasty wire was passed through the small opening and advanced into the LCA and distal to the aorta. An angioplasty balloon along the wire was then pushed forward and inflated with 12 atmospheric pressure followed by dilatation within the arteries. In sham-operated control (SC) animals, only skin and muscle layers were opened followed by closing these two layers.

Animals were categorized into group 1 (SC), group 2 (BDLCCAE), group 3 [BDLCCAE + ESRD on regulatory hemodialysis patient's serum [i.e., mixed together serum from three patients (1 cc/injection into deprived CA adventitia, i.e., the adventitial layer of LCCA was carefully removed)], group 4 [BDLCCAE + ESRD patient's serum (1 cc/injection from peri-adventitial layer)], and group 5 [BDLCCAE + ESRD patient's serum (2 cc/by intravenous injection at days 1, 3, 7, 10 and 14 after BDLCCADE)] and the LCCA was harvested by day-21 after BDLCCAE procedure.

Cell culturing for assessing the impact of p-Cresol on upregulating oxidative stress, inflammation and cell apoptosis, and downregulated angiogenesis in human umbilical vein endothelial cells

The methodology has been mentioned in detail our previous study [35]. Human umbilical vein endothelial cells (HUVECs) were purchased from the BCRC (Taiwan) and the culture medi-

um was bought from ScienCell. In our *in vitro* investigation, the groups were categorized into group A: p-Cresol (50 μM) (i.e., uremic toxic substance stimulation) + HUVECs; and group B being the control group (i.e., HUVECs with culture medium only). The cells were continuously cultured in M199 culture medium for six hours before being collected for individual analysis. The dosage of p-Cresol was based on our previous report [36].

Measurement of LCCA contractility, vasorelaxation and nitric oxide (NO) release

At the end of study, LCCA was isolated, cleaned, and cut into slices of 2 mm in length for evaluating contractile and relaxant responses as previously reported [35]. The carotid rings were carefully mounted on an isometric force transducer with a tension of 1.8 g and placed in an organ chamber filled with Krebs solution maintained at pH 7.4 and bubbled with 95% O_2 and 5% CO_2. After an equilibration of 40 minutes, 1 μM of phenylephrine (PE) was added to the organ chamber for the assessment of contractile activity, and then 30 μM of acetylcholine (ACh) was added to assess endothelial integrity. All data were acquired and analyzed using the DMT system.

Carotid arterial-based nitric oxide release was estimated as % difference between PE-induced vasocontraction response in the presence and absence of L-NAME that has been reported in our previous study [35]. Additionally, the Griess Reagent System (Promega, G2930) was utilized for measuring the production of NO from LCCA.

Assessment of rodent carotid arterial angiogenetic ability

The methodology has been reported in our previous study [35]. Briefly, the animal carotid arterial angiogenetic capacity was evaluated in twenty-four well-culture plates that were mosaiced with one hundred and fifty microliter of 1 mg/mL type-I collagen (BD Biosciences) and permitted to gel for sixty min. at 37°C and five % CO_2. Photographs were performed on 1st day and the twelfth day with 12.5 × magnification. The number and length of sprouting microvasculature (i.e., angiogenesis) were analyzed by ULYMPUS DP72 software. Experiments were carried two times.

Matrigel analysis for human umbilical vein endothelial cell angiogenetic capacity

The procedure and protocol have been described by our previous report [37]. After 6-hours incubation, images of the network generated from tube formation were retrieved using an inverted phase-contrast microscope (Olympus IX51) and quantified by WimTube.

H.E. stain for morphometric analysis of LCA

The procedure and protocol have been described in our previous studies [35]. At day twenty-one after the endothelial cell damage, the LCA in every rodent was obtained; the cross-sections of denudated LCA were stained with H.E and were morphometrically calculated by a computer-analysis system. For each rat, the section of damaged vessel was analyzed. The areas of lumen, the internal elastic lamina (IEL), neointima of IEL, and medial layer (i.e., external EL) were analyzed. The intimal region was defined as the luminal surface and IEL.

To assess ROS generation in the total cells and mitochondrial compartment

Carboxy-H_2DCFDA (Invitrogen) was used to examine intra-cellular ROS production. Carboxy-H_2DCFDA dye was diluted in Phosphate-Buffered Saline at a concentration of ten mM and the plates hold in a 37°C, five % CO_2 incubator for thirty min. After incubation, the dye solution was eliminated, and the cells washed with Phosphate-Buffered Saline and furthermore cultured for thirty min in fully defined cultured-medium. For analyses of mitochondrial ROS in cells, the MitoSOX™ Red dye was directly replenished at a concentration of ten nM for a more thirty min incubation. Fluorescence intensity was assessed by Beckman Coulter Cytomics FC 500 Flow Cytometer.

Western blot analysis

The procedure and protocol for Western blot analysis have been described in our previous studies [17, 18, 22, 23]. Equal amounts (50 μg) of protein extracts were separated by SDS-PAGE and the separated proteins transferred onto a polyvinylidene difluoride (PVDF) membrane (Amersham Biosciences, Amersham, UK). Nonspecific sites were blocked by

incubation of the membrane in blocking buffer [5% nonfat dry milk in T-TBS (TBS containing 0.05% Tween 20)] at room temperature for 1 hour. Then the membranes were incubated with the indicated primary antibodies for 1 hour at room temperature. After washing, immunoreactive membranes were visualized by enhanced chemiluminescence and exposed to Biomax L film.

Immunofluorescent (IF) staining

The procedure and protocol of IF staining were based on our previous reports [17, 18, 22, 23]. In detail, for IF staining, rehydrated paraffin sections were first treated with 3% H_2O_2 for 10 minutes and incubated with Immuno-Block reagent (BioSB, Santa Barbara, CA, USA) for 30 minutes at room temperature. Sections were then incubated with primary antibodies, while sections incubated with the use of irrelevant antibodies served as controls. Three sections of brain specimen from each rat were analyzed. For quantification, three randomly selected HPFs (200 × or 400 × for IHC and IF studies) were analyzed in each section. The mean number of positive-stained cells per HPF for each animal was then determined by summation of all numbers divided by 9.

Statistical analysis

The data were shown as means ± SD. Statistical analysis was carried using analysis of variance, then by Bonferroni multiple comparison. SAS statistical software for Windows version 8.2 (SAS institute, Cary, NC, USA) was used. A p value < 0.05 was viewed statistically significant.

Results

*p-Cresol enhanced the protein expressions of oxidative stress and inflammation in HUVECs (**Figure 1**)*

To elucidate whether p-Cresol would upregulate the expression of oxidative stress biomarkers in HUVECs, Western blotting was performed. The results showed that the protein expression of NOX-1, NOX-2, oxidized protein and p22phox (**Figure 1A-D**), four indicators of oxidative stress, were significantly increased in p-Cresol treated HUVECs (group A) than in control group (i.e., HUVECs without treatment) (group B).

Next, by using the same tool, we tested whether the inflammatory biomarkers in HUVECs would be upregulated by p-Cresol treatment. As expected, the protein expressions of IL-1β, TNF-α and IL-6 (**Figure 1E-G**), three indicators of inflammation, were significantly increased in group A than group B. These findings implicated that uremic toxic substance (i.e., p-Cresol) would enhance the generation of oxidative stress and inflammatory reaction in endothelial cells (i.e., HUVECs).

*p-Cresol enhanced the protein expressions of apoptosis and autophagy in HUVECs (**Figure 2**)*

Further, we performed Western blotting to assess the protein levels of apoptotic and autophagic biomarkers in HUVECs undergoing p-Cresol treatment. As per our hypothesis, the protein expression of mitochondrial Bax, cleaved caspase 3 and cleaved PARP (**Figure 2A-C**), three indicators of apoptosis were significantly upregulated in group A than in group B. Consistently, the protein expressions of beclin, Atg5 and ratio of protein LC3B-II to protein LC3B-I (**Figure 2D-F**), three indices of autophagic biomarkers, displayed a similar pattern to apoptosis between the two groups, highlighting that p-Cresol treatment augmented HUVEC damage and death.

*p-Cresol enhanced oxidative stress in whole cells and mitochondria, and DNA damage in HUVECs (**Figure 3**)*

To assess oxidative stress at the cellular level when undergoing p-Cresol treatment, flow cytometric analysis was performed. The result showed the fluorescent intensity of Mitosox in HUVECs, an indicator of mitochondrial level of oxidative stress, was significantly increased in group A than in group B (**Figure 3A**, **3B**). Additionally, fluorescent intensity of H2DCFDA in HUVECs, an indicator of intracellular oxidative stress, exhibited an identical pattern to Mitosox between the two groups (**Figure 3C**, **3D**).

Further, the IF microscopic finding of TUNEL assay demonstrated that the number of apop-

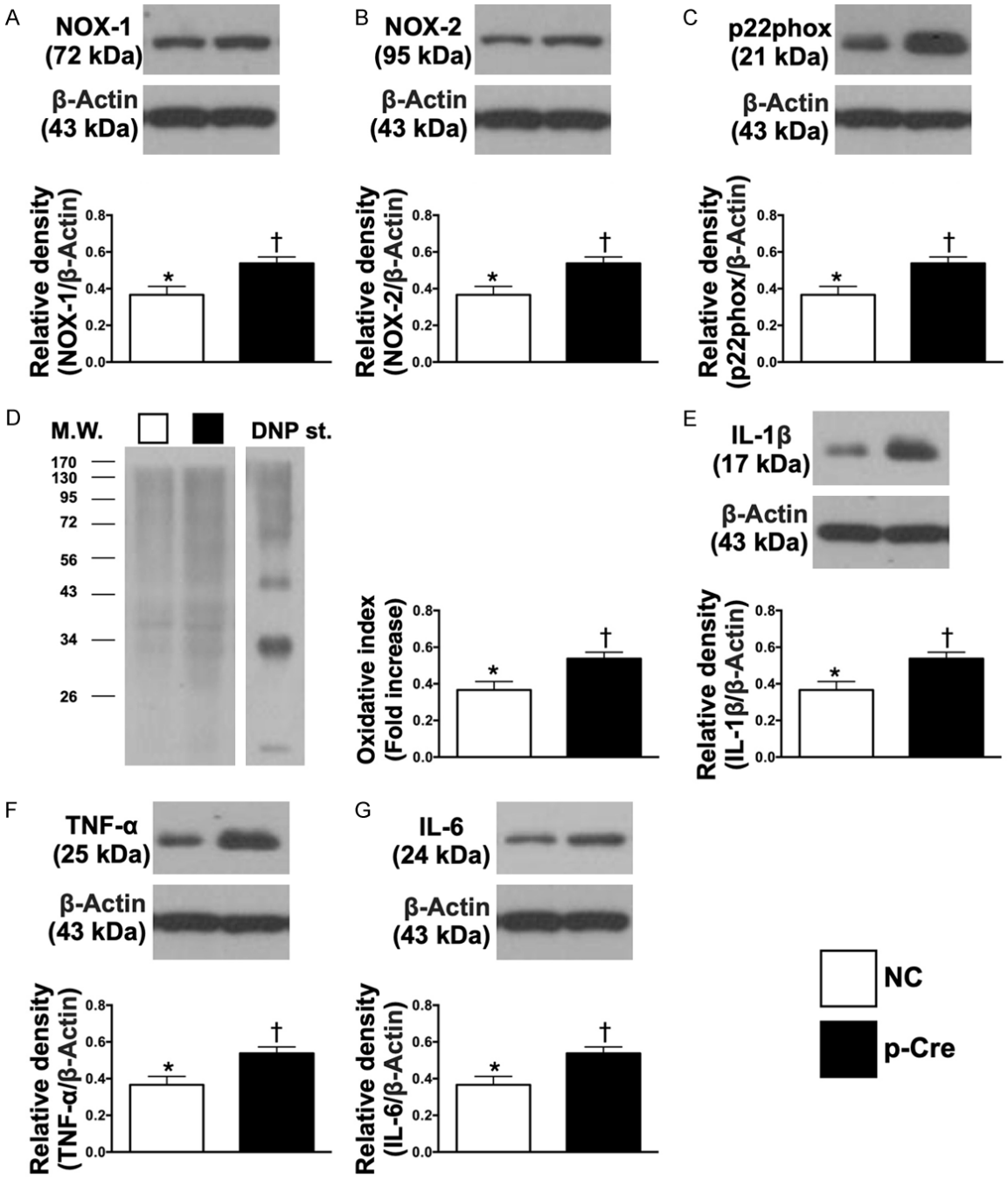

Figure 1. p-Cresol treatment augmented the protein expressions of oxidative stress and inflammation in HUVECs. A. Protein expression of NOX-1, * vs. †, P < 0.01. B. Protein expression of NOX-2, * vs. †, p < 0.01. C. Protein expression of p22phox, * vs. †, P < 0.01. D. Oxidized protein expression, * vs. †, P < 0.01. (Note: left and right lanes shown on the upper panel represent protein molecular weight marker and control oxidized molecular protein standard, respectively). M.W = molecular weight; DNP = 1-3 dinitrophenylhydrazone. E. Protein expressions of interleukin (IL)-1β, * vs. †, P < 0.001. F. Protein expression of tumor necrosis factor (TNF)-α, * vs. †, P < 0.01. G. Protein expression of IL-6, * vs. †, P < 0.01. NC = normal control; p-Cre = p-Cresol; HUVECs = human umbilical vein endothelial cells. n = 4 in each group.

totic nuclei in HUVECs displayed a similar pattern of oxidative stress between group A and group B (**Figure 3E**, **3F**). Our findings suggested that p-Cresol treatment promoted oxidative stress and apoptosis in the endothelial cells.

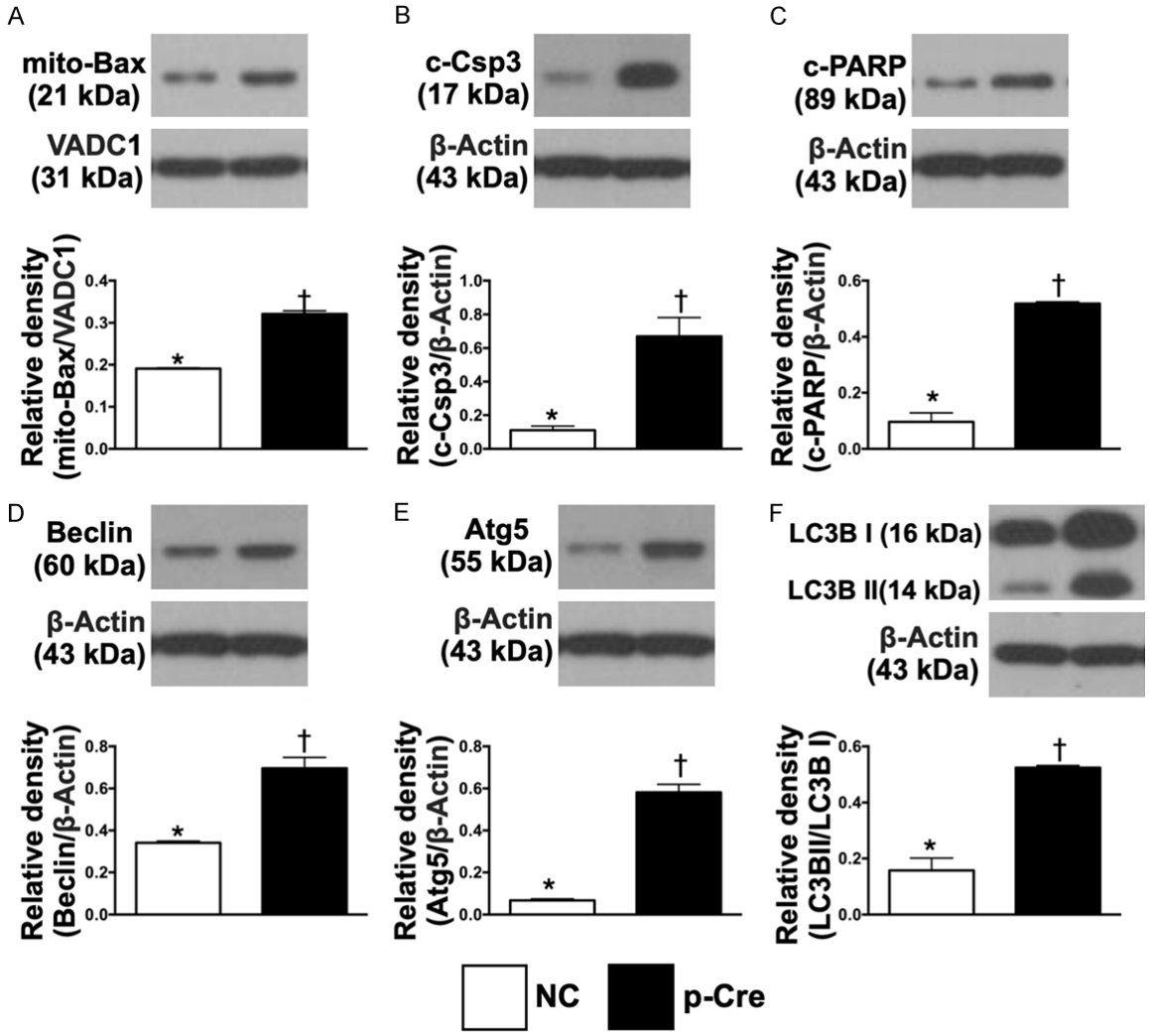

Figure 2. p-Cresol enhanced the protein expressions of apoptosis and autophagy in HUVECs. A. Protein expression of mitochondrial (mito)-Bax, * vs. †, P < 0.01. B. Protein expression of cleaved caspase 3 (c-Csp3), * vs. †, P < 0.001. C. Protein expression of cleaved Poly (ADP-ribose) polymerase (c-PARP), * vs. †, P < 0.001. D. Protein expressions of beclin, * vs. †, P < 0.001. E. Protein expression of Atg5, * vs. †, P < 0.001. F. Ratio of protein LC3B-II to protein LC3B-I, * vs. †, P < 0.001. NC = normal control; p-Cre = p-Cresol; HUVECs = human umbilical vein endothelial cells. n = 4 in each group.

*p-Cresol suppressed angiogenesis (**Figure 4**)*

To test whether p-Cresol treatment would inhibit angiogenesis, Matrigel assay was done to determine the ability of HUVEC to perform angiogenesis. The result showed the capacity of angiogenesis was significantly lower in p-Cresol treated HUVECs than in control group HUVECs (**Figure 4A-F**).

For further assessment of angiogenesis, we utilized rat carotid ring undergoing culture and this ex vivo study was categorized into five groups as: group 1 (SC), group 2 [balloon injured (i.e., denuded endothelial cells) carotid artery (BICA)], group 3 [BICA + ESRD serum (1 cc/injection from deprivation of adventitia layer of CA)], group 4 [BICA + ESRD serum (1 cc/injection from peri-adventitia layer of CA for one time)], and group 5 [BICA + ESRD serum (2 cc/by intravenous injection at days 1, 3, 7, 10 and 14 after)], respectively. The result showed that the angiogenesis capacity of carotid ring was significantly progressively reduced from groups 1 to 5 (**Figure 4G**, **4H**).

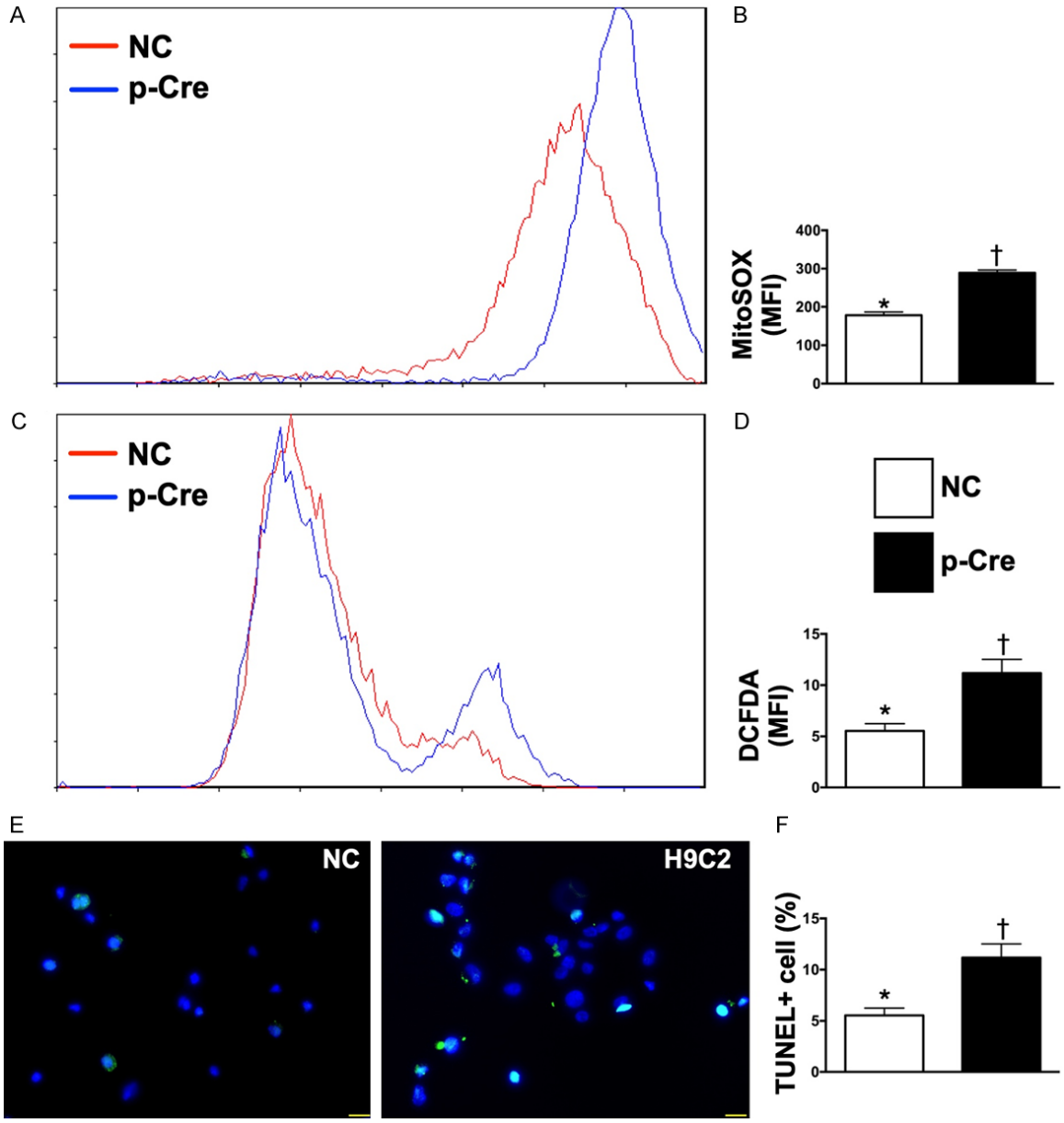

Figure 3. p-Cresol enhanced oxidative stress in whole cells and mitochondria and DNA damage in HUVECs. A. Illustrating flow cytometric analysis for mitochondrial level of oxidative stress with HUVECs stained by MitoSOX. B. Analytical result of fluorescent intensity of MitoSOX in HUVEC mitochondria, * vs. †, $P < 0.001$. C. Illustrating flow cytometric analysis for identification of intracellular oxidative stress with HUVECs stained by H2DCFDA. D. Analytical result of fluorescent intensity of H2DCFDA in HUVECs, * vs. †, $P < 0.001$. E. Illustrating microscopic finding (400 ×) of TUNEL assay for identification of apoptotic nuclei of HUVECs (green color). Scale bars in the right lower corner represent 20 μm. F. Analytical result of number of apoptotic nuclei, * vs. †, $P < 0.001$. NC = normal control; p-Cre = p-Cresol; HUVECs = human umbilical vein endothelial cells; MFI = mean fluorescent intensity. n = 5 in each group.

*Carotid artery relaxation and NO release (**Figure 5**)*

By using the Griess Reagent System, we observed that the NO expression of denuded LCCA significantly and progressively reduced from groups 1 to 5 (**Figure 5D**). Baseline NO release from endothelial cells of denuded LCCA also exhibited an identical pattern as detected by Griess Reagent System among the five groups (**Figure 5A**).

Furthermore, to elucidate the impact of uremic toxic substances on regulating vessel relax-

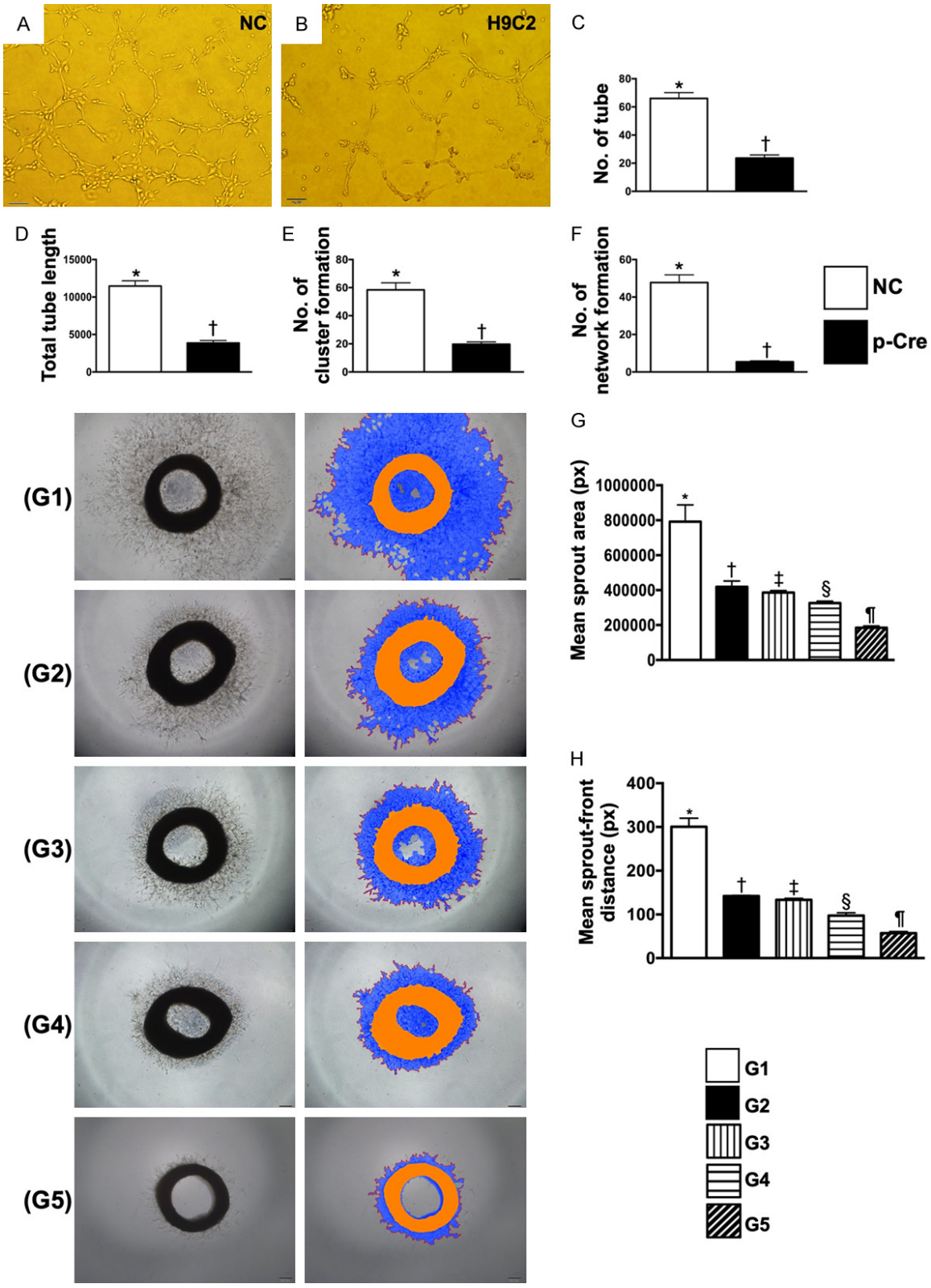

Figure 4. p-Cresol suppressed angiogenesis of HUVECs and carotid ring. A, B. Illustrating the *in vitro* study of Matrigel assay for assessment of angiogenesis (n = 6). C. Number of tubules, * vs. †, P < 0.00001. D. Tubular length, * vs. †, P < 0.0001. E. Number of cluster formation, * vs. †, P < 0.0001. F. Number of network formation, * vs. †, P < 0.0001. (Group 1 to Group 5) Illustrating the exo vivo study of carotid-ring angiogenesis (n = 4). G. Analytical result of mean sprout area, * vs. other groups with different symbols (†, ‡, §, ¶), P < 0.0001. H. Analytical result of

mean sprout-front distance, * vs. other groups with different symbols (†, ‡, §, ¶), P < 0.0001. Group 1 = SC; Group 2 = balloon denuded left common carotid artery endothelium (BDLCCAE); Group 3 = BDLCCAE + end stage renal disease (ESRD) patient's serum (i.e., mixed serum from 3 patients) [(1 cc/injection from deprivation of adventitia layer of left common carotid artery (LCCA) for one time]; Group 4 [BDLCCAE + ESRD patient's serum (1 cc/injection from peri-adventitia layer of LCCA for one time)]; Group 5 [BDLCCAE + ESRD patient's serum (2 cc/by intravenous injection at days 1, 3, 7, 10 and 14 after BDLCCAE procedure)]. All statistical analyses were performed by one-way ANOVA, followed by Bonferroni multiple comparison post hoc test (n = 4 or 6 for each group). Symbols (*, †, ‡, §, ¶) indicate significance (at 0.05 level).

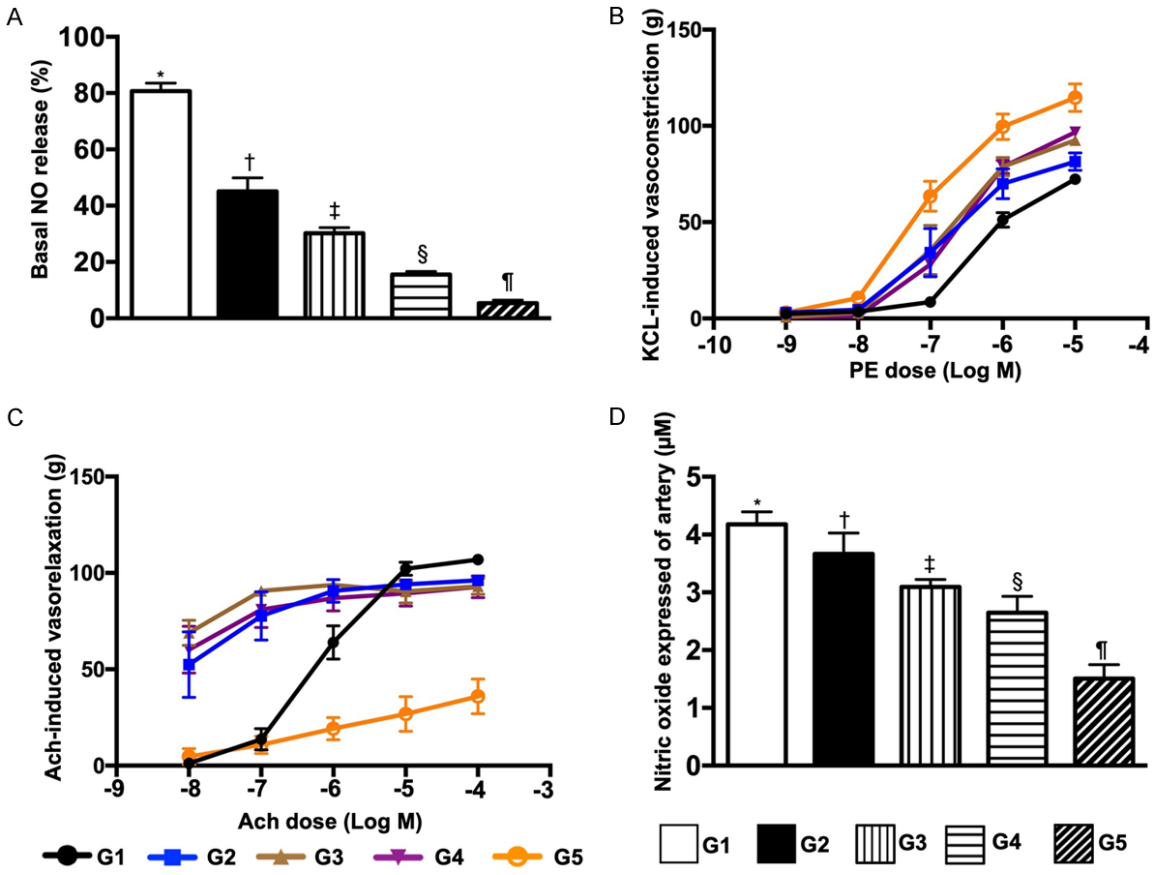

Figure 5. Exo vivo study of carotid vasorelaxation and nitric oxide (NO) release by day 21 after balloon denuded LCCA. A. Schematic illustration of NO release from denuded endothelial cells of LCCA was significantly progressively decreased from groups 1 to 5. Additionally, NO-release was especially impaired in groups 4 and 5 than in group 1. Analytical result of NO release (%) among the five groups, * vs. other groups with different symbols (†, ‡, §, ¶), P < 0.0001. B. Conversely, phenylephrine (PE)-induced vasoconstriction progressively increased from groups 1 to 5. Analytical result of vasoconstriction (%), * vs. other groups with different symbols (†, ‡, §, ¶) (i.e., among Group 1 to Group 5), P < 0.0001. C. Ach-induced vasorelaxation significantly and progressively reduced from groups 1 to 5. Analytical result of vasorelaxation (%), * vs. other groups with different symbols (†, ‡, §, ¶) (i.e., among Group 1 to Group 5), P < 0.0001. D. Analytical result of NO expression in LCCA (μM), * vs. other groups with different symbols (†, ‡, §, ¶), P < 0.0001. All statistical analyses were performed by one-way ANOVA, followed by Bonferroni multiple comparison post hoc test (n = 6 for each group). Symbols (*, †, ‡, §, ¶) indicate significance (at 0.05 level). LCCA = left common carotid artery. NO = nitric oxide.

ation and contraction, denuded LCCA was cut into pieces and mounted on the machine system. As expected, vasoconstriction (**Figure 5B**) significantly and progressively increased, whereas vasorelaxation (**Figure 5C**) significantly and progressively reduced from groups 1 to 5.

*Uremic toxic substances induced carotid artery hyperplasia by day 21 after endothelial denudation by angioplasty balloon (**Figure 6**)*

To elucidate the impact of serum derived from an ESRD patient on carotid arterial hyperplasia,

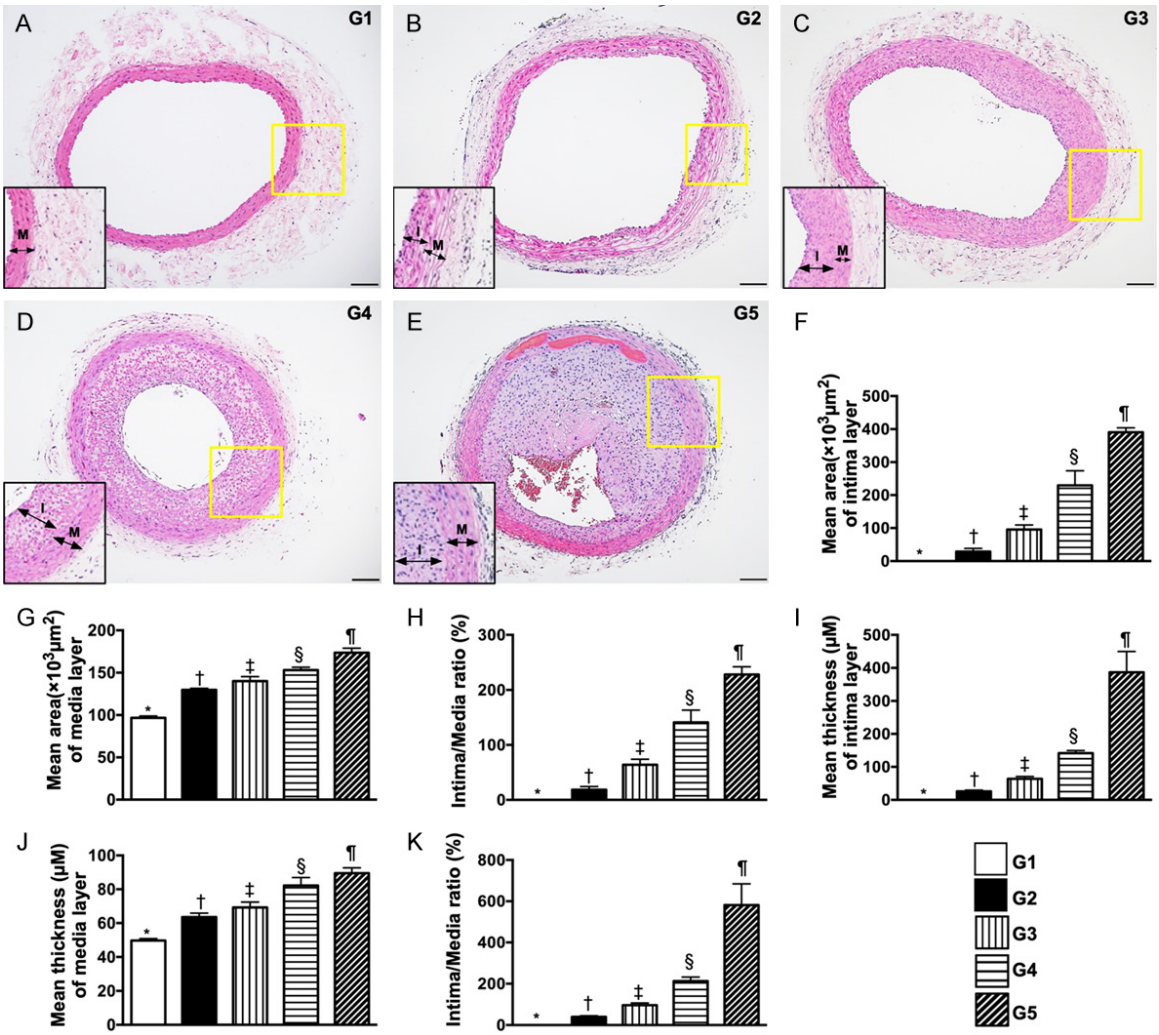

Figure 6. Microscopic identification of uremic toxic substances induced neointimal and medial layer proliferations by day 21 after balloon denuded LCCA. A-E. Illustrating microscopic finding (100 ×) of H & E staining for identification of the proliferations of intimal and medial layers of LCCA. The black line of square box indicated the manifestation of yellow line small square box. I = intimal layer; M = medial layer. F. Analytic result of intimal area (i.e., area of neointimal proliferation), * vs. other groups with different symbols (†, ‡, §, ¶), $P < 0.0001$. G. Analytical result of medial area, * vs. other groups with different symbols (†, ‡, §), $P < 0.001$. H. Analytical result of ratio of mean medial-layer area to mean intimal-layer area, * vs. other groups with different symbols (†, ‡, §, ¶), $P < 0.0001$. I. Mean of three cross sections of intimal layer thickness, * vs. other groups with different symbols (†, ‡, §, ¶), $P < 0.0001$. J. Mean of three cross sections of medial layer thickness, * vs. other groups with different symbols (†, ‡, §, ¶), $P < 0.0001$. K. Analytical result of ratio of mean thickness of intimal layer to mean thickness of medial layer, * vs. other groups with different symbols (†, ‡, §, ¶), $P < 0.0001$. Scale bars in right lower corner represent 100 μm. All statistical analyses were performed by one-way ANOVA, followed by Bonferroni multiple comparison post hoc test (n = 6 for each group). Symbols (*, †, ‡, §, ¶) indicate significance (at 0.05 level). LCCA = left common carotid artery.

we denuded the endothelium of rat LCCA by coronary angioplasty balloon (1.5 × 15 mm size) inflations three times up to 14 atmospheric pressure at the common carotid artery (**Figure 6A-E**). The result demonstrated that the internal cross section of carotid artery was significantly and progressively reduced from groups 1 to 5 (**Figure 6F**), whereas the intimal and medial layer and thickness of carotid artery were significantly and progressively increased from groups 1 to 5 (**Figure 6G-K**), suggesting that serum uremic toxic substances increased hyperplasia and proliferation of intimal and smooth muscle layers of carotid artery after endothelial denudation, resulting in carotid artery obstruction. Of particularly im-

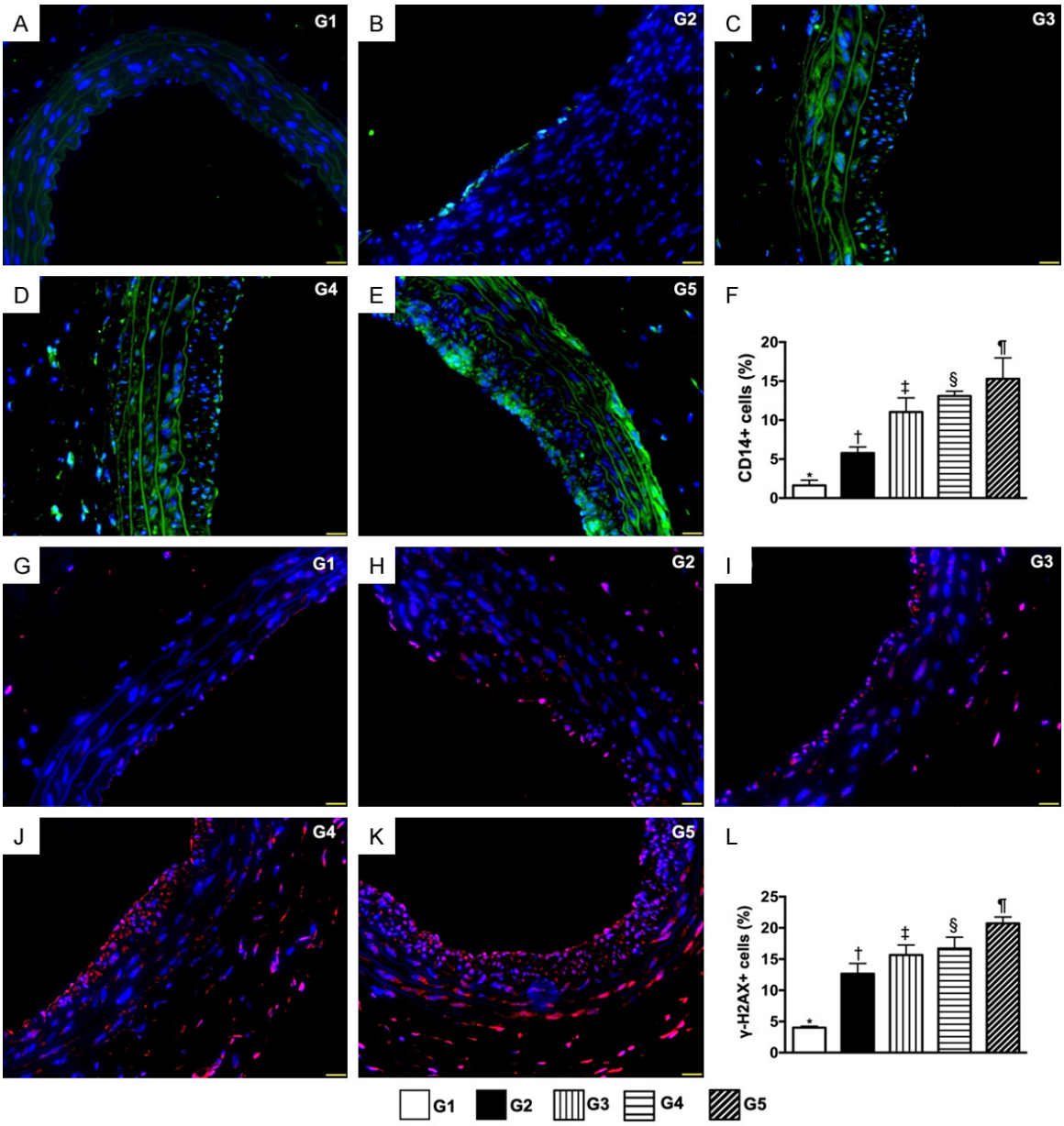

Figure 7. Uremic toxic substances enhanced inflammatory cell infiltration and DNA-damaged biomarker in carotid artery by day 21 after endothelial denudation by angioplasty balloon. A-E. Immunofluorescent (IF) microscopic finding (400 ×) for identification of positively stained CD14 cells (green color). F. Analytical result of number of CD14+ cells, * vs. other groups with different symbols (†, ‡, §, ¶), P < 0.0001. G-K. IF microscopic finding (400 ×) for identification of positively stained γ-H2AX cells (red color). L. Analytical result of number of γ-H2AX+ cells, * vs. other groups with different symbols (†, ‡, §, ¶), P < 0.0001. Scale bars in right lower corner represent 20 μm. All statistical analyses were performed by one-way ANOVA, followed by Bonferroni multiple comparison post hoc test (n = 6 for each group). Symbols (*, †, ‡, §, ¶) indicate significance (at 0.05 level).

portant finding was that these parameters were significantly less severe in group 3 (i.e., deprivation of adventitia layer) than in group 4, implicating that adventitia layer played an essentially accessory role on enhancing the proliferation/hyperplasia of intimal and medial layers undergoing the uremic-toxic substance treatment.

*Uremic toxic substances enhanced inflammatory cell infiltration and DNA-damaged biomarker in carotid artery by day 21 after endothelial denudation by angioplasty balloon (**Figure 7**)*

The cellular expression of CD14 (**Figure 7A-E**), an indicator of inflammation, was significantly

and progressively upregulated from groups 1 to 5 (**Figure 7F**). Additionally, the cellular expression of γ-H2AX (**Figure 7G-K**), an indicator of DNA-damage, displayed an identical pattern of inflammation between the two groups (**Figure 7L**).

*Uremic toxic substances suppressed expressions of endothelial cells and enhanced the expression of EPC in carotid artery by day 21 after endothelial denudation by angioplasty balloon (**Figure 8**)*

The cellular expression of vWF (**Figure 8A-E**), which is an indicator of endothelial functional integrity, significantly and progressively decreased from groups 1 to 5 (**Figure 8F**). Conversely, the cellular expression of CXCR4 (**Figure 8G-K**), an indicator of EPC, significantly and progressively increased from groups 1 to 5, suggesting an intrinsic response for repairing the endothelial lineage after endothelial cell damage by balloon and further damage by balloon + uremic toxic substances (**Figure 8L**).

Discussion

Plentiful data have previously identified that atherosclerosis results from the initiation and propagation of endothelial dysfunction [1-4]. Additionally, our previous studies [36, 38] have shown that p-Cresol, an essential uremic toxic substance, upregulated the ROS-inflammatory signaling pathway in rat renal tubular cells and cardiomyocytes. Consistently, the present study also displayed that, compared with HUVECs only, the inflammatory, oxidative-stress (i.e., including total intracellular and mitochondrial levels) apoptotic and autophagic biomarkers were increased, whereas angiogenesis capacity was reduced in HUVECs after receiving p-Cresol treatment. Our findings therefore corroborate with the findings of previous studies [14, 36, 38] and highlight that uremic toxic substances played a principal role in endothelial dysfunction and damage.

Intriguingly, previous studies have demonstrated that resident stem cells and some inflammatory cells are embryologically present in the adventitia and participate in vascular-wall remodeling in response to damaged vessel stimulation [29, 30], resulting in neointimal/smooth muscle cell proliferation and, ultimately, arteriosclerosis [31-33]. An essential finding in the present study was that as compared with group 1 (SC) the carotid-ring formation of angiogenesis (i.e., ex vivo study) was substantially reduced in group 2 (BDLCCAE) and was more substantially reduced in group 4 [BDLCCAE + ESRD patient's serum (1 cc) injected from periadventitial layer)]. However, as compared with group 4 this angiogenesis ability was preserved in group 3 [BDLCCAE + ESRD patient's serum (1 cc) injected into deprived CA adventitia]. Additionally, LCCA remodeling (i.e., thickness of intimal and medial layers resultant from hyperplasia, proliferation and stenosis; i.e., narrower LCCA luminal area) as well as inflammatory cell infiltration (i.e., positively stained CD14+ and F4/80+ cells) exhibited an identical pattern to carotid-ring angiogenesis among the groups 1 to 4. In this way, our findings enriched those of previous studies [29-33] and yielded several preclinically relevant implications: (1) uremic toxic substances were involved in suppression of angiogenesis and enhancement of inflammatory reaction in LCCA; (2) the adventitial layer facilitated uremic toxic substances to participate in LCCA remodeling and obstruction (3) that were attenuated by deprivation of the adventitial layer.

A principal finding in the ex vivo study was that, as compared to group 1, the vasorelaxation of denuded LCCA was reduced in group 2, more substantially reduced in group 4, and was partially reversed in group 3 as compared with group 4. Conversely, NO-release in denuded LCCA displayed an opposite pattern to vasorelaxation among the four groups. Our findings once again demonstrated that uremic toxic substances played a crucial role and the adventitial layer of LCCA acted as a key complementary role on LCCA-wall remodeling and stenosis. Another principal finding in the present study was that the number of positively stained CD31 and vWF cells in LCCA, two indicators of endothelial lineage integrity, was significantly and progressively reduced from groups 1 to 4. This may explain the phenomenon of defective vasorelaxation and NO release in denuded LCCA among the groups.

The most important finding in the present study was that, as compared with groups 1 to 4, intravenous injection of uremic toxic substances in group 5 played an extremely important role in remodeling, stenosis and molecular-cellular perturbations in denuded LCCA. Our findings can now explain why previous clinical studies

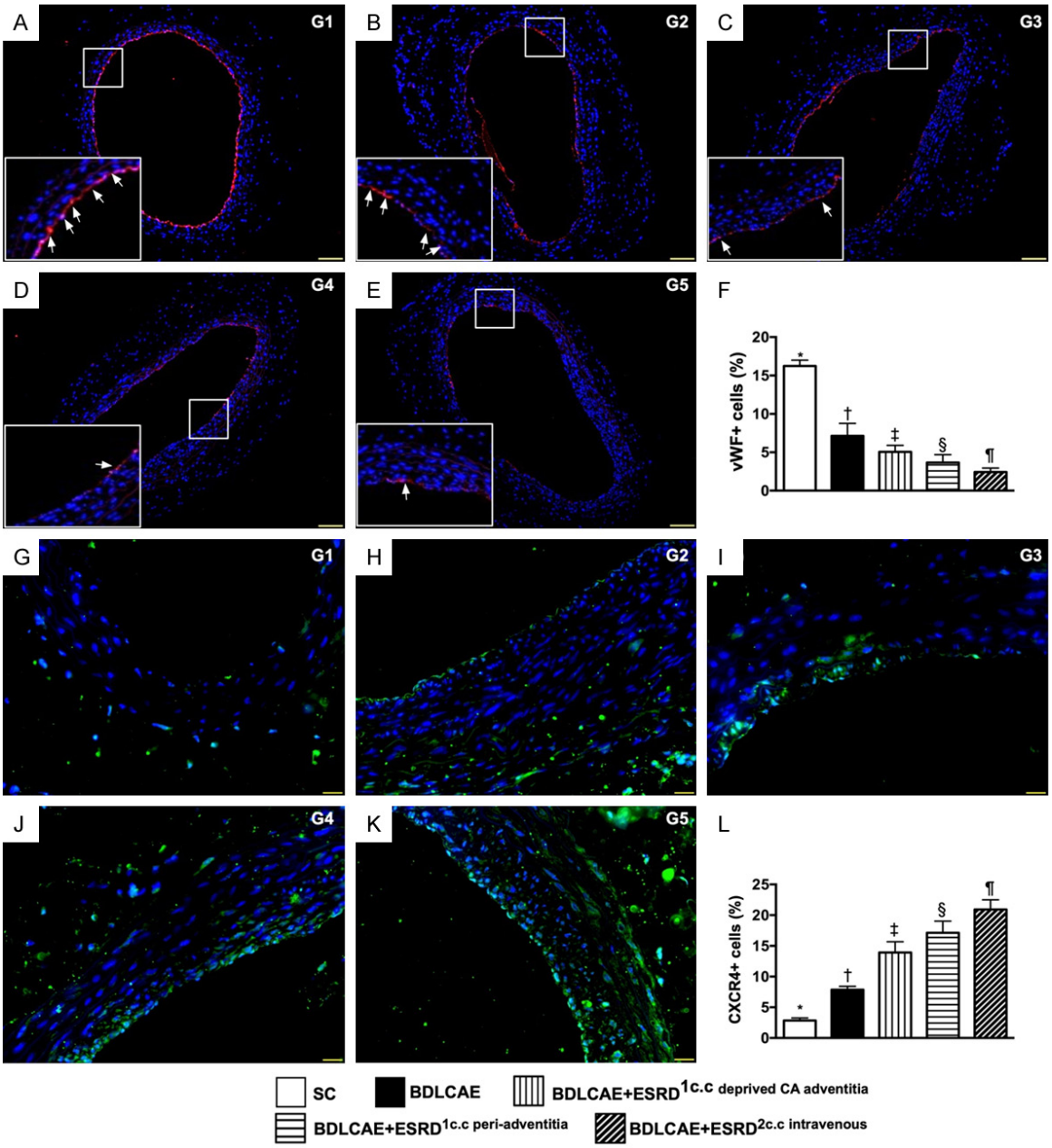

Figure 8. Uremic toxic substances suppressed expressions of endothelial cells endothelial progenitor cells in carotid artery by day 21 after endothelial denudation by angioplasty balloon. A-E. Immunofluorescent (IF) microscopic finding (400 ×) for identification of positively stained von Willebrand factor (vWF) cells (red color). F. Analytical result of number of vWF+ cells, * vs. other groups with different symbols (†, ‡, §, ¶), $P < 0.0001$. G-K. IF microscopic finding (400 ×) for identification of positively stained CXCR4 cells (green color). L. Analytical result of number of CXCR4+ cells, * vs. other groups with different symbols (†, ‡, §, ¶), $P < 0.0001$. Scale bars in right lower corner represent 20 μm. All statistical analyses were performed by one-way ANOVA, followed by Bonferroni multiple comparison post hoc test (n = 6 for each group). Symbols (*, †, ‡, §, ¶) indicate significance (at 0.05 level).

have demonstrated that uremic toxic substances are one of the most harmful factors to cause endothelial dysfunction and plaque formation but also cause AOS [12, 13] with very poor response to medication and coronary artery interventions [13-21], resulting in unfavorable long-term prognosis [19-22].

Study limitations

This study has limitations. First, we did not define the exact components of the uremic toxic substances derived from each ESRD patient's serum. Accordingly, we do not know which component was the most essential for

induction of denuded LCCA remodeling and stenosis. Second, we did not perform a stepwise concentration increase of uremic toxic substances on denuded LCCA. Accordingly, without dosage titrations, we did not conclude the optimal concentration/volume of uremic toxic serum for inducing denuded LCCA remodeling and stenosis in rat.

In conclusion, uremic toxic substances played an essential role in vascular wall remodeling and obstruction, and the adventitial layer played a complementary role in initiation and propagation of atherosclerosis.

Acknowledgements

This study was supported by a program grant from Chang Gung Memorial Hospital, Chang Gung University (Grant number: CMRPG8G-0911).

Disclosure of conflict of interest

None.

Address correspondence to: Dr. Jun Guo, Department of Cardiology, The First Affiliated Hospital, Ji'nan University, 613 W. Huangpu Avenue, Guangzhou 510630, China. E-mail: dr.guojun@163.com; Dr. Hon-Kan Yip, Division of Cardiology, Department of Internal Medicine, Kaohsiung Chang Gung Memorial Hospital and Chang Gung University College of Medicine, 123 Dapi Road, Niaosung District, Kaohsiung 83301, Taiwan. Tel: +886-7-7317123 Ext. 8300; Fax: +886-7-7322402; E-mail: han.gung@msa.hinet.net

References

[1] Ross R. The pathogenesis of atherosclerosis: a perspective for the 1990s. Nature 1993; 362: 801-809.

[2] Harrison DG. Endothelial dysfunction in atherosclerosis. Basic Res Cardiol 1994; 89 Suppl 1: 87-102.

[3] Sanders M. Molecular and cellular concepts in atherosclerosis. Pharmacol Ther 1994; 61: 109-153.

[4] Ross R. Atherosclerosis–an inflammatory disease. N Engl J Med 1999; 340: 115-126.

[5] Ross R. The arterial wall and atherosclerosis. Annu Rev Med 1979; 30: 1-15.

[6] Selwyn AP, Vita JA, Vekshtein VI, Yeung A, Ryan T Jr and Ganz P. Myocardial ischemia: pathogenic role of disturbed vasomotion and endothelial dysfunction in coronary atherosclerosis. Adv Cardiol 1990; 37: 42-52.

[7] Falk E, Shah PK and Fuster V. Coronary plaque disruption. Circulation 1995; 92: 657-671.

[8] Burke AP, Farb A, Malcom GT, Liang YH, Smialek J and Virmani R. Coronary risk factors and plaque morphology in men with coronary disease who died suddenly. N Engl J Med 1997; 336: 1276-1282.

[9] Bhatt DL, Steg PG, Ohman EM, Hirsch AT, Ikeda Y, Mas JL, Goto S, Liau CS, Richard AJ, Rother J, Wilson PW and Investigators RR. International prevalence, recognition, and treatment of cardiovascular risk factors in outpatients with atherothrombosis. JAMA 2006; 295: 180-189.

[10] Chen C, Wei J, AlBadri A, Zarrini P and Bairey Merz CN. Coronary microvascular dysfunction-epidemiology, pathogenesis, prognosis, diagnosis, risk factors and therapy. Circ J 2016; 81: 3-11.

[11] Poorzand H, Tsarouhas K, Hozhabrossadati SA, Khorrampazhouh N, Bondarsahebi Y, Bacopoulou F, Rezaee R, Jafarzadeh Esfehani R and Morovatdar N. Risk factors of premature coronary artery disease in Iran: a systematic review and meta-analysis. Eur J Clin Invest 2019; 49: e13124.

[12] Collins AJ, Foley RN, Herzog C, Chavers B, Gilbertson D, Herzog C, Ishani A, Johansen K, Kasiske B, Kutner N, Liu J, St Peter W, Ding S, Guo H, Kats A, Lamb K, Li S, Li S, Roberts T, Skeans M, Snyder J, Solid C, Thompson B, Weinhandl E, Xiong H, Yusuf A, Zaun D, Arko C, Chen SC, Daniels F, Ebben J, Frazier E, Hanzlik C, Johnson R, Sheets D, Wang X, Forrest B, Constantini E, Everson S, Eggers P and Agodoa L. US renal data system 2012 annual data report. Am J Kidney Dis 2013; 61: A7, e1-476.

[13] Cai Q, Mukku VK and Ahmad M. Coronary artery disease in patients with chronic kidney disease: a clinical update. Curr Cardiol Rev 2013; 9: 331-339.

[14] Sarnak MJ, Levey AS, Schoolwerth AC, Coresh J, Culleton B, Hamm LL, McCullough PA, Kasiske BL, Kelepouris E, Klag MJ, Parfrey P, Pfeffer M, Raij L, Spinosa DJ and Wilson PW; American Heart Association Councils on Kidney in Cardiovascular Disease, High Blood Pressure Research, Clinical Cardiology, and Epidemiology and Prevention. Kidney disease as a risk factor for development of cardiovascular disease: a statement from the American Heart Association Councils on Kidney in Cardiovascular Disease, High Blood Pressure Research, Clinical Cardiology, and Epidemiology and Prevention. Hypertension 2003; 42: 1050-65.

[15] Collins AJ, Foley RN, Chavers B, Gilbertson D, Herzog C, Johansen K, Kasiske B, Kutner N, Liu J, St Peter W, Guo H, Gustafson S, Heubner B, Lamb K, Li S, Li S, Peng Y, Qiu Y, Roberts T, Skeans M, Snyder J, Solid C, Thompson B, Wang C, Weinhandl E, Zaun D, Arko C, Chen

SC, Daniels F, Ebben J, Frazier E, Hanzlik C, Johnson R, Sheets D, Wang X, Forrest B, Constantini E, Everson S, Eggers P and Agodoa L. United states renal data system 2011 annual data report: atlas of chronic kidney disease & end-stage renal disease in the United States. Am J Kidney Dis 2012; 59: A7, e1-420.

[16] Yahalom G, Kivity S, Segev S, Sidi Y and Kurnik D. Estimated glomerular filtration rate in a population with normal to mildly reduced renal function as predictor of cardiovascular disease. Eur J Prev Cardiol 2014; 21: 941-948.

[17] Ohtake T, Kobayashi S, Moriya H, Negishi K, Okamoto K, Maesato K and Saito S. High prevalence of occult coronary artery stenosis in patients with chronic kidney disease at the initiation of renal replacement therapy: an angiographic examination. J Am Soc Nephrol 2005; 16: 1141-1148.

[18] Cooper WA, O'Brien SM, Thourani VH, Guyton RA, Bridges CR, Szczech LA, Petersen R and Peterson ED. Impact of renal dysfunction on outcomes of coronary artery bypass surgery: results from the society of thoracic surgeons national adult cardiac database. Circulation 2006; 113: 1063-1070.

[19] Hillis GS, Croal BL, Buchan KG, El-Shafei H, Gibson G, Jeffrey RR, Millar CG, Prescott GJ and Cuthbertson BH. Renal function and outcome from coronary artery bypass grafting: impact on mortality after a 2.3-year follow-up. Circulation 2006; 113: 1056-1062.

[20] Nakayama Y, Sakata R, Ura M and Itoh T. Long-term results of coronary artery bypass grafting in patients with renal insufficiency. Ann Thorac Surg 2003; 75: 496-500.

[21] Wellenius GA, Mukamal KJ, Winkelmayer WC and Mittleman MA. Renal dysfunction increases the risk of saphenous vein graft occlusion: results from the Post-CABG trial. Atherosclerosis 2007; 193: 414-420.

[22] Herzog CA, Ma JZ and Collins AJ. Poor long-term survival after acute myocardial infarction among patients on long-term dialysis. N Engl J Med 1998; 339: 799-805.

[23] Yeh KH, Sheu JJ, Lin YC, Sun CK, Chang LT, Kao YH, Yen CH, Shao PL, Tsai TH, Chen YL, Chua S, Leu S and Yip HK. Benefit of combined extracorporeal shock wave and bone marrow-derived endothelial progenitor cells in protection against critical limb ischemia in rats. Crit Care Med 2012; 40: 169-177.

[24] Losordo DW, Henry TD, Davidson C, Sup Lee J, Costa MA, Bass T, Mendelsohn F, Fortuin FD, Pepine CJ, Traverse JH, Amrani D, Ewenstein BM, Riedel N, Story K, Barker K, Povsic TJ, Harrington RA and Schatz RA; ACT34-CMI Investigators. Intramyocardial, autologous CD34+ cell therapy for refractory angina. Circ Res 2011; 109: 428-436.

[25] Lee FY, Chen YL, Sung PH, Ma MC, Pei SN, Wu CJ, Yang CH, Fu M, Ko SF, Leu S and Yip HK. Intracoronary transfusion of circulation-derived CD34+ cells improves left ventricular function in patients with end-stage diffuse coronary artery disease unsuitable for coronary intervention. Crit Care Med 2015; 43: 2117-2132.

[26] Ueno H, Koyama H, Fukumoto S, Tanaka S, Shoji T, Shoji T, Emoto M, Tahara H, Tsujimoto Y, Tabata T and Nishizawa Y. Dialysis modality is independently associated with circulating endothelial progenitor cells in end-stage renal disease patients. Nephrol Dial Transplant 2010; 25: 581-586.

[27] Chen YT, Cheng BC, Ko SF, Chen CH, Tsai TH, Leu S, Chang HW, Chung SY, Chua S, Yeh KH, Chen YL and Yip HK. Value and level of circulating endothelial progenitor cells, angiogenesis factors and mononuclear cell apoptosis in patients with chronic kidney disease. Clin Exp Nephrol 2013; 17: 83-91.

[28] Lee MS, Lee FY, Chen YL, Sung PH, Chiang HJ, Chen KH, Huang TH, Chen YL, Chiang JY, Yin TC, Chang HW and Yip HK. Investigated the safety of intra-renal arterial transfusion of autologous CD34+ cells and time courses of creatinine levels, endothelial dysfunction biomarkers and micro-RNAs in chronic kidney disease patients-phase I clinical trial. Oncotarget 2017; 8: 17750-17762.

[29] Hu Y and Xu Q. Adventitial biology: differentiation and function. Arterioscler Thromb Vasc Biol 2011; 31: 1523-1529.

[30] Torsney E and Xu Q. Resident vascular progenitor cells. J Mol Cell Cardiol 2011; 50: 304-311.

[31] Orlandi A. The contribution of resident vascular stem cells to arterial pathology. Int J Stem Cells 2015; 8: 9-17.

[32] Zhang L, Issa Bhaloo S, Chen T, Zhou B and Xu Q. Role of resident stem cells in vessel formation and arteriosclerosis. Circ Res 2018; 122: 1608-1624.

[33] Yu B, Chen Q, Le Bras A, Zhang L and Xu Q. Vascular stem/progenitor cell migration and differentiation in atherosclerosis. Antioxid Redox Signal 2018; 29: 219-235.

[34] Shao PL, Chiu CC, Yuen CM, Chua S, Chang LT, Sheu JJ, Sun CK, Wu CJ, Wang CJ and Yip HK. Shock wave therapy effectively attenuates inflammation in rat carotid artery following endothelial denudation by balloon catheter. Cardiology 2010; 115: 130-144.

[35] Lee FY, Sun CK, Sung PH, Chen KH, Chua S, Sheu JJ, Chung SY, Chai HT, Chen YL, Huang TH, Huang CR, Li YC, Luo CW and Yip HK. Daily melatonin protects the endothelial lineage and functional integrity against the aging process, oxidative stress, and toxic environment and re-

stores blood flow in critical limb ischemia area in mice. J Pineal Res 2018; 65: e12489.
[36] Chua S, Lee FY, Chiang HJ, Chen KH, Lu HI, Chen YT, Yang CC, Lin KC, Chen YL, Kao GS, Chen CH, Chang HW and Yip HK. The cardioprotective effect of melatonin and exendin-4 treatment in a rat model of cardiorenal syndrome. J Pineal Res 2016; 61: 438-456.
[37] Huang TH, Sun CK, Chen YL, Wang CJ, Yin TC, Lee MS and Yip HK. Shock wave enhances angiogenesis through VEGFR2 activation and recycling. Mol Med 2017; 22: 850-862.
[38] Zhen YY, Yang CC, Hung CC, Lee CC, Lee CC, Wu CH, Chen YT, Chen WY, Chen KH, Yip HK and Ko SF. Extendin-4 protects kidney from acute ischemia-reperfusion injury through upregulation of NRF2 signaling. Am J Transl Res 2017; 9: 4756-4771.